

Coherent data transmission with microresonator Kerr frequency combs

Joerg Pfeifle,¹ Matthias Lauermann,¹ Daniel Wegner,¹ Victor Brasch,² Tobias Herr,²
 Klaus Hartinger,³ Jingshi Li,¹ David Hillerkuss,^{1,4} Rene Schmogrow,¹ Ronald Holzwarth,^{3,5}
 Wolfgang Freude,^{1,6} Juerg Leuthold,^{1,6,4} T. J. Kippenberg,² and Christian Koos^{1,6,*}

¹*Institute of Photonics and Quantum Electronics (IPQ),*

Karlsruhe Institute of Technology (KIT), 76131, Karlsruhe, Germany

²*École Polytechnique Fédérale de Lausanne (EPFL), 1015, Lausanne, Switzerland*

³*Menlo Systems GmbH, 82152 Martinsried, Germany*

⁴*now with ETH Zurich, 8092 Zurich, Switzerland*

⁵*Max-Planck-Institut für Quantenoptik, 85746 Garching, Germany*

⁶*Institute of Microstructure Technology (IMT), Karlsruhe Institute of Technology (KIT), 76131, Karlsruhe, Germany*

Optical frequency combs enable coherent data transmission on hundreds of wavelength channels and have the potential to revolutionize terabit communications [1]. Generation of Kerr combs in nonlinear integrated microcavities [2] represents a particularly promising option enabling line spacings of tens of GHz, compliant with wavelength-division multiplexing (WDM) grids [3]. However, Kerr combs may exhibit strong phase noise and multiplet spectral lines [4–6], and this has made high-speed data transmission impossible up to now. Recent work has shown that systematic adjustment of pump conditions enables low phase-noise Kerr combs with singlet spectral lines [4, 7–9]. Here we demonstrate that Kerr combs are suited for coherent data transmission with advanced modulation formats that pose stringent requirements on the spectral purity of the optical source. In our experiment, we encode a data stream of 392 Gbit/s on subsequent lines of a Kerr comb using quadrature phase shift keying (QPSK) and 16-state quadrature amplitude modulation (16QAM). The results demonstrate that Kerr combs can meet the highly demanding requirements of multi-terabit/s coherent communications and thus offer a solution towards chip-scale terabit/s transceivers.

Optical interconnects providing multi-terabit/s data rates are the most promising option to overcome transmission bottlenecks in warehouse-scale data centres and world-wide communication networks. By using highly parallel wavelength division multiplexing (WDM) with tens or hundreds of channels in combination with spectrally efficient advanced modulation formats, multi-terabit/s transmission capacity can be achieved while keeping symbol rates compliant with the electrical bandwidth of energy-efficient CMOS driver circuitry [10, 11]. The silicon platform allows for co-integration of photonic and electronic circuitry using fabless CMOS processing [12, 13]. While integrated terabit/s WDM receivers have already been demonstrated [14], scalability of the transmitter capacity is still limited by the lack of adequate optical sources, especially when using advanced modulation formats that encode information on both the amplitude and the phase of the optical wave and therefore require optical carriers with particularly low phase and amplitude noise.

Optical carriers for WDM transmission are commonly generated by distributed feedback (DFB) laser arrays. Chip-scale transmitter systems with DFB lasers have been realized on indium phosphide (InP) substrates, showing potential for simultaneous operation of 40 channels [15]. However, these approaches cannot be directly

transferred to the silicon photonic platform: Combining conventional DFB laser arrays with silicon photonic transmitters would require a multitude of chip-chip interfaces, increasing significantly the packaging effort. Hybrid integration of III-V dies on silicon substrates [16, 17] avoids these interfaces, but scalability to large channel counts is still limited by the gain bandwidth of the semiconductor material and by thermal constraints. Moreover, spectral efficiency of DFB-based transmission systems suffers from the uncertainty of the individual emission frequencies, which is of the order of several GHz and requires appropriate guard bands to avoid spectral overlap of neighbouring WDM channels. For dense WDM with a channel spacing of, e.g., 25 GHz, the guard bands consume a significant fraction of the available transmission bandwidth.

These limitations can be overcome by exploiting optical frequency combs as sources for WDM transmission. Frequency combs consist of a multitude of equidistant spectral lines, each of which can be individually modulated [1, 21, 22]. The inherently constant frequency spacing of the comb lines enables transmission of orthogonal frequency division multiplexing (OFDM) signals [1] or of Nyquist-WDM signals [23] with closely spaced subcarriers. Frequency combs with line spacings in the GHz range can be generated by external modulation of a narrowband continuous-wave signal [24], by mode-locked lasers based on semiconductor quantum-dot or quantum-dash materials [25], or by exploiting parametric frequency conversion in Kerr-nonlinear high-Q microcavities [2]. In contrast to

*Electronic address: christian.koos@kit.edu

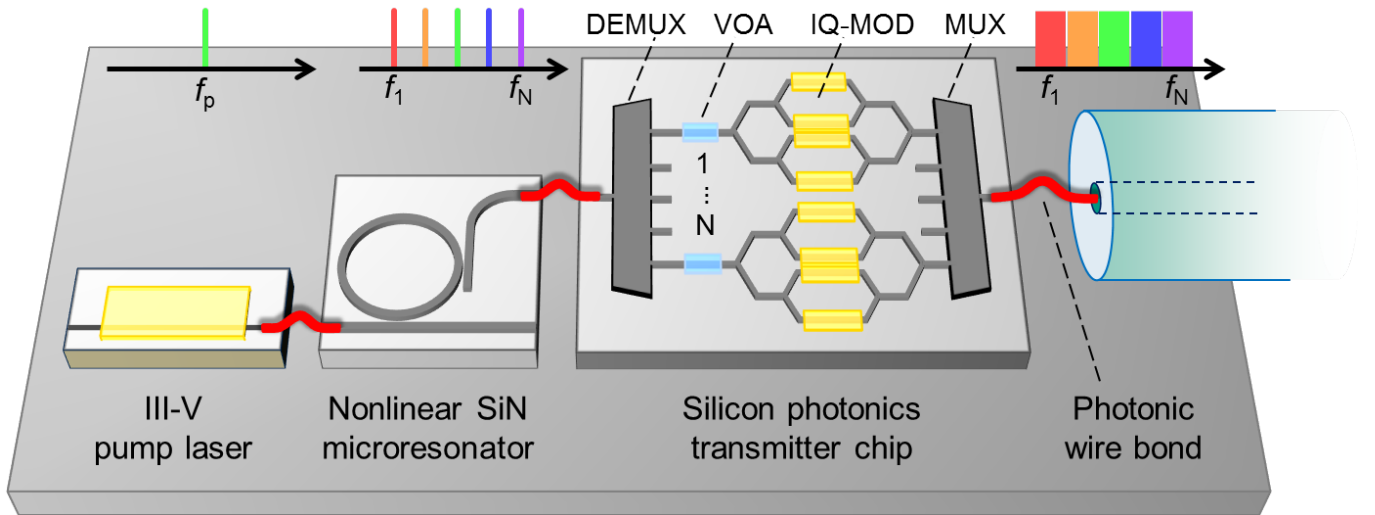


FIG. 1: **Artist's view of a chip-scale terabit/s transmitter.** The system combines silicon photonic transmitter circuitry with a Kerr frequency comb acting as an optical source for WDM transmission. For Kerr comb generation, a narrowband continuous-wave III-V laser pumps a high-Q silicon nitride microresonator. Resonant enhancement of the optical field in the presence of Kerr nonlinearity leads to formation of a frequency comb comprising a multitude of optical carriers at equidistant frequencies $f_1 \dots f_N$; the associated spectra are depicted above the respective component. A WDM demultiplexer (DEMUX) separates the comb lines, and variable optical attenuators (VOA) are used to adjust the power of the individual carriers. Data are encoded on the in-phase and quadrature component by electro-optical modulators (IQ-MOD), and the data streams are combined by a WDM multiplexer (MUX). Proper pulse shaping techniques enable a densely packed optical signal spectrum which is schematically depicted in the upper right. Photonic wire bonds [18] connect the individual chips and link up the transmission fibre, thus enabling an efficient combination of different photonic integration platforms in a multi-chip assembly. The feasibility of the various silicon photonic passive components and electro-optic modulators has been shown [12, 19, 20]. The demonstration of coherent data transmission with Kerr combs is the subject of this work.

modulator-based approaches or mode-locked laser diodes, the bandwidth of Kerr combs is neither limited by the achievable modulation depth nor by the gain bandwidth of the active medium. Kerr combs can hence exhibit bandwidths of hundreds of nanometers [26], thereby covering multiple telecommunication bands (such as the C, L, and U band) with typical line spacings between 10 GHz and 100 GHz.

Kerr comb generation has been demonstrated using various different technology platforms [26] such as silica [2], calcium fluoride (CaF_2) [27], Hydex glass [28] or silicon nitride (Si_3N_4) [29]. Previous experiments have used such devices for data transmission with conventional 10 Gbit/s or 40 Gbit/s on-off-keying as a modulation format [3, 5, 6]. However, Kerr frequency combs tend to exhibit multiplet spectral lines within a single resonance leading to strong amplitude fluctuations and phase noise [4, 5]. Such fluctuations are prohibitive for spectrally efficient data transmission with advanced modulation formats. While low phase-noise Kerr combs have been demonstrated recently [4, 7–9], coherent transmission with Kerr combs has not yet been shown.

Here we report on the first experimental demonstration of coherent data transmission with amplitude- and phase-modulated carriers derived from a Kerr frequency comb [30]. Coherent transmission allows to increase the information content and to boost the data rate, but also

places stringent requirements on the phase and amplitude stability of the optical carrier. Our experiments build on systematic investigations of comb formation dynamics [4] to generate highly stable Kerr combs with low phase noise. We encode uncorrelated data on neighbouring comb lines using quadrature phase shift keying (QPSK) and 16-state quadrature amplitude modulation (16QAM) in combination with Nyquist pulses that have nearly rectangular power spectra and enable highest spectral efficiency. Using polarization multiplexing and a symbol rate of 14 GBd on five QPSK and one 16QAM channel, we obtain an aggregate data rate of 392 Gbit/s. This corresponds to a net spectral efficiency of 6 bit/s/Hz (3 bit/s/Hz) for the 16QAM (QPSK) channels. The results clearly demonstrate the large potential of Kerr frequency combs for future chip-scale terabit/s communication systems. We choose silicon nitride as a reliable integration platform which is compatible with CMOS processing [29, 31].

The vision of a chip-scale terabit/s transmitter is illustrated in Fig. 1. A Kerr frequency comb is generated by exploiting multi-stage four-wave mixing in a high-Q Kerr-nonlinear microresonator that is pumped with a strong continuous-wave (cw) laser [2, 26]. The envisaged transmitter consists of a multi-chip assembly, where single-mode photonic wire bonds [18] connect the individual chips. In contrast to monolithic integration this hybrid

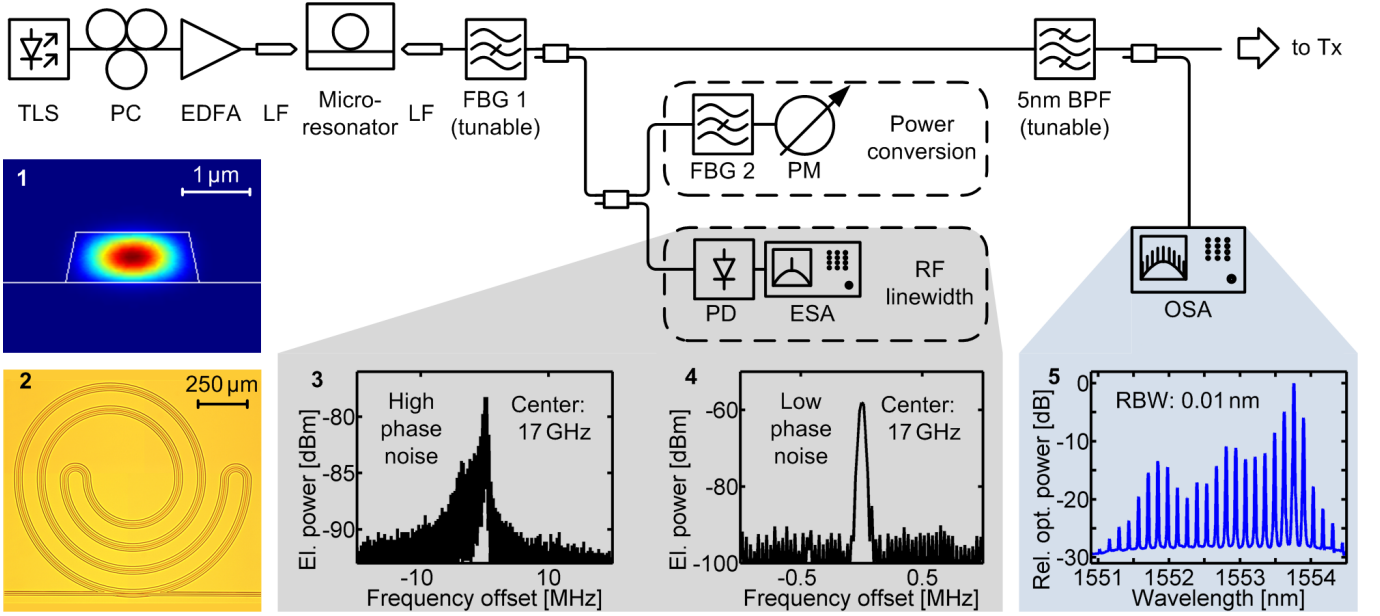


FIG. 2: Comb-generation setup. The optical pump comprises a tunable laser source (TLS), a polarization controller (PC), and an erbium-doped fibre amplifier (EDFA). Lensed fibres (LF) are used to couple light to and from the microresonator chip. The microresonator consists of a Si_3N_4 waveguide which is approximately $2\ \mu\text{m}$ wide and $750\ \text{nm}$ high with sidewalls inclined by 12° with respect to the vertical direction. The waveguide cross section and the mode profile (for a bend radius of $1.35\ \text{mm}$) are depicted in Inset 1. The ring resonator has a spiral-like layout to decrease the footprint and to reduce stitching errors during electron beam lithography, see Inset 2. After the microresonator, a fibre Bragg grating (FBG 1) serves as a tunable narrowband notch filter to suppress the residual pump light. For adjustment of the pump parameters, we monitor the power conversion from the pump to the adjacent lines. An electronic spectrum analyser (ESA) is used to measure the RF linewidth in the photocurrent spectrum of the photodetector (PD). When tuning into a low phase-noise comb state, the RF spectrum switches from a broad band (Inset 3, RBW $10\ \text{kHz}$) to a single narrow line (Inset 4, RBW $30\ \text{kHz}$). A $5\ \text{nm}$ wide spectral section is extracted from the comb spectrum and used for data transmission (Inset 5). The pump wavelength and on-chip pump power are $1549.4\ \text{nm}$ and $33\ \text{dBm}$, respectively.

approach allows to combine the advantages of different photonic integration platforms: For the optical pump, III-V semiconductors can be used [15], while the high-Q ring resonator for Kerr comb generation could be fabricated using, e. g., low-loss silicon-nitride waveguides [29]. The optical carriers are separated and individually modulated on a silicon photonic chip, for which large-scale silicon photonic integration lends itself to realize particularly compact and energy-efficient MUX and DEMUX filters [12] and IQ modulators [19, 20].

The viability of the concept illustrated in Fig. 1 is demonstrated in a proof-of-principle experiment with discrete photonic components. Kerr combs are generated with the setup depicted in Fig. 2. A narrow-linewidth tunable pump laser source (TLS) is adjusted in polarization and amplified by an erbium-doped fibre amplifier (EDFA). Lensed fibres (LF) couple light to a Si_3N_4 ring resonator with a free spectral range (FSR) of $17\ \text{GHz}$, Fig. 2. Inset 1 shows the waveguide cross section of the ring and the calculated mode profile. The ring resonator waveguide is coiled up to reduce the footprint and thereby the stitching errors during electron beam lithography (Fig. 2, Inset 2). In contrast to the concept illustrated in Fig. 1, our experiment, relies on a comb generator with a

single waveguide which is used both to couple pump light to the resonator and to extract the frequency comb. As a consequence, strong cw pump light can pass through the resonator and needs to be suppressed by a tunable fibre Bragg grating (FBG 1) at the output of the device. It has recently been shown that stability and phase noise of the Kerr comb are closely linked to the pump conditions [4]. Careful tuning of pump power, frequency, and polarization is therefore of prime importance. To adjust these parameters in the experiment we used two optimization criteria: First, we measure the power conversion from the pump to all newly generated comb lines using a power meter (PM) after a second fibre Bragg grating (FBG 2) that completely blocks the pump. Second, we record the radio-frequency (RF) power spectrum of the photocurrent that is generated by direct detection of the comb. If the pump parameters are correctly adjusted, a single narrowband line in the photodetector current spectrum is expected, indicating that the comb consist of equidistant narrowband spectral lines, see Fig. 2, Inset 4. Otherwise, if the lines are not frequency-locked, or if multiplet spectra exist, a broadband RF spectrum is observed, (Fig. 2, Inset 3). Further details of the adjustment procedure can be found in the Methods Section.

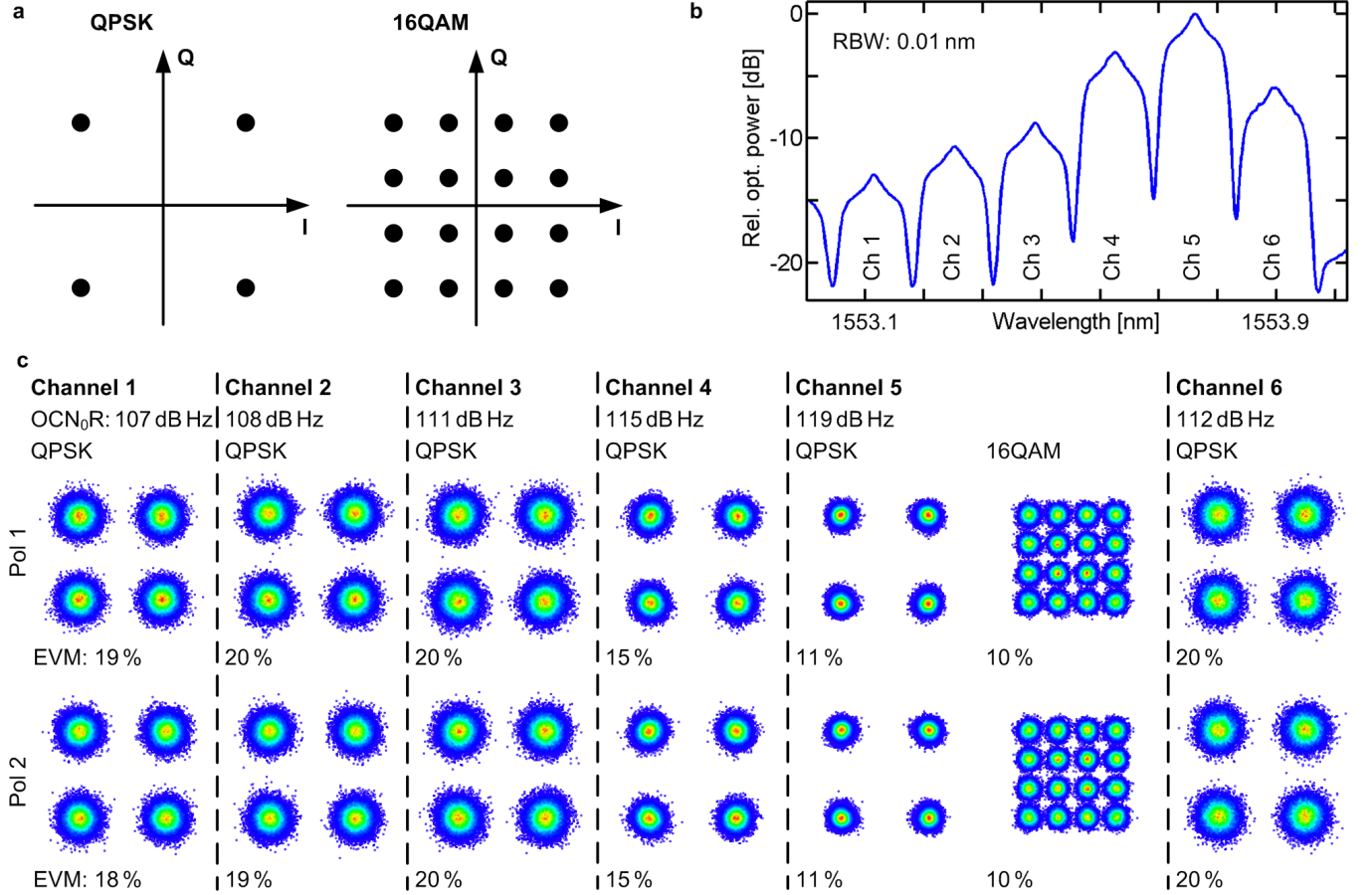


FIG. 3: **Coherent data transmission using a Kerr microresonator frequency comb.** **a**, Constellation diagrams of QPSK and 16QAM signals. Information is encoded both on the amplitude and the phase of the optical carrier, which can be represented by the in-phase (I, horizontal axis) and the quadrature component (Q, vertical axis) of the complex electrical field. Each point in the constellation diagram corresponds to a complex symbol that represents 2 (4) bits of information for the case of QPSK (16QAM). **b**, Spectrum of modulated carriers for all six data channels, measured at the input of the optical modulation analyser (OMA). **c**, Constellation diagrams for each channel and for both polarizations along with the corresponding error vector magnitude (EVM) and the optical carrier-to-noise-density ratio (OCN₀R). The constellation diagrams show no sign of excessive phase noise, which would result in constellation points that are elongated along the azimuthal direction. For QPSK the BER of all channels is below 10^{-3} , which corresponds to an EVM of 32 %; for channels 4 and 5 the BER is even smaller than 10^{-9} (EVM < 17 %). The good quality of channel 5 enables transmission of a 16QAM signal with a measured BER of 7.5×10^{-4} .

For data transmission, a 5 nm wide spectral section (Fig. 2, Inset 5) is extracted from the comb using an optical band-pass filter (BPF). The carriers are modulated with QPSK and 16QAM signals at a symbol rate of 14 GBd. To enable dense packing of optical channels and to maximize the spectral efficiency, we used sinc-shaped Nyquist pulses with rectangular power spectra [32]. We transmit data streams on two orthogonal polarizations of a standard single-mode fibre (polarization-division multiplexing). The signal is detected with a commercial optical modulation analyser using a tunable laser as a local oscillator. The experimental setup for data transmission and the digital post-processing techniques are described in more detail in the Supplementary Information.

The results of the data transmission experiment are

summarized in Fig. 3. For the case of QPSK and 16QAM information is encoded both on the amplitude and the phase of the optical carrier. The received complex electric field is visualized by its in-phase (I, horizontal axis) and quadrature component (Q, vertical axis) in the complex plane, Fig. 3a. For QPSK, the I and the Q-component can assume two distinct values, leading to four signal states (symbols) in the complex plane. This represents an information content of two bits per symbol. Likewise, a 16QAM symbol can assume 16 states in the complex plane, corresponding to four bits of information per symbol. Fig. 3b depicts the optical power spectrum of the modulated carriers for all six data channels. We did not flatten the comb spectrum prior to modulation for comparing the influence of different carrier powers on

the transmission performance. As a quantitative measure of the signal quality, we use the error vector magnitude (EVM), which describes the effective distance of a received complex symbol from its ideal position in the constellation diagram. The EVM is directly connected to the bit-error ratio (BER) if the signal is impaired by additive white Gaussian noise only [33]. The constellation diagrams for each polarization of the six wavelength channels are depicted in Fig. 3c along with the measured EVM. When using second-generation forward-error correction (FEC) with 7 % overhead, the BER limits for error-free detection are given by 10^{-3} [34]. For QPSK, this corresponds to an EVM threshold of 32 %, which is well above the measured EVM for all channels, indicating that error-free transmission is possible. For 16QAM, requirements are more stringent, and an EVM of 11 % is needed for error-free transmission. This is fulfilled for channel 5, which shows a measured BER of 7.5×10^{-4} . We transmit with a symbol rate of 14 GBd and choose QPSK for channels 1...4 and 6, and 16QAM for channel 5. Taking into account polarization multiplexing, we obtain an aggregate data rate of 392 Gbit/s. Considering the overhead of 7 % for second generation FEC, the net spectral efficiency amounts to 3 bit/s/Hz for the QPSK and to 6 bit/s/Hz for the 16QAM channels.

When relating the EVM to the BER, we assume that the signal is impaired by additive white Gaussian noise. The validity of this assumption is supported by the fact that the deviations of the measured from the ideal constellation points occur equally in all directions and do not show any sign of anisotropy. Excessive phase noise, in particular, can be excluded as a relevant impairment of data transmission as this would lead to constellation points which are elongated along the azimuthal direction. The results indicate that Kerr combs are indeed perfectly suited for data transmission with phase-sensitive modulation formats.

The remaining signal impairments can be attributed to strong amplified spontaneous emission (ASE) originating from the high-power pump EDFA. In the current configuration, the ASE light passes straight through the resonator chip and superimposes the comparatively weak comb lines as additive white Gaussian noise. The power of the comb lines is limited by the efficiency of the frequency conversion and the coupling of the pump to the resonator.

As a figure of merit we define the optical carrier-to-noise-density ratio (OCN_0R), which relates the power of the unmodulated carrier to the underlying noise power in a spectral bandwidth of 1 Hz, see Methods Section for more details. In our experiment, the OCN_0R is correlated to the EVM: For channel 5, we obtain a good OCN_0R of more than 119 dB Hz, which enables a very good QPSK signal and a good 16QAM signal. Channel 4 with an OCN_0R of more than 115 dB Hz still gives a very good QPSK signal but lacks performance for 16QAM. Channels 1...3 as well as channel 6 exhibit even lower OCN_0R resulting in larger EVM figures. There are var-

ious options to improve the OCN_0R , e.g., by coupling a second waveguide to the microresonator to extract the comb while suppressing ASE noise, see Methods Section for a more detailed discussion. This gives room for future improvement of the transmission performance.

In summary we demonstrate that Kerr frequency combs are well suited for high-capacity data transmission with phase-sensitive modulation formats. We show error-free transmission of a 392 Gbit/s data stream using six neighbouring WDM channels with QPSK and 16QAM modulation formats. The received signals exhibit no sign of excessive phase noise, and there is significant potential to further improve the optical carrier-to-noise-density ratio of the Kerr comb. Assuming that the demonstrated spectral efficiency of 6 bit/s/Hz can be maintained over the entire bandwidth of the Kerr comb, we envision chip-scale transmitters providing aggregate data rates beyond 100 Tbit/s, only limited by nonlinear effects in the single-mode silica fibres used for transmission [35]. In the long run, these limitations might even be overcome by mode division multiplexing based on, e.g., exploiting the orbital angular momentum (OAM) of the fiber modes to create orthogonal data streams [36]. The combination of chip-scale Kerr frequency comb sources with large-scale silicon photonic integration could hence become a key concept for power-efficient optical interconnects providing transmission rates that have hitherto been considered impossible.

Acknowledgements

This work was supported by the European Research Council (ERC Starting Grant 'EnTeraPIC', number 280145), by the Alfred Krupp von Bohlen und Halbach Foundation, by Helmholtz International Research School for Teratronics (HIRST), by the Initiative and Networking Fund of the Helmholtz Association, by the Center for Functional Nanostructures (CFN) of the Deutsche Forschungsgemeinschaft (DFG) (project A 4.8), by the DFG Major Research Instrumentation Programme, by the Karlsruhe Nano-Micro Facility (KNMF), by the Karlsruhe School of Optics & Photonics (KSOP), by the Swiss National Science Foundation (NCCR Nano-Tera, NTF MCOMB), by a Marie Curie IAPP Action and by the DARPA program QuASAR. Samples have been fabricated at the EPFL Center for Micro- and Nanotechnology (CMI).

Methods

Experimental setup and ring resonator design.

The pump for Kerr comb generation is generated by an external-cavity laser (New Focus Velocity Model TLB-6728), a polarization controller (PC) and an erbium-doped fibre amplifier (EDFA) providing an output power

of up to 37 dBm, see Fig. 2. The coupling loss between the lensed fibre and the Si_3N_4 chip amounts to approximately 3 dB per facet. In the data transmission experiment we pump a resonance near 1549.4 nm with an on-chip power of approximately 33 dBm. The tunable fibre Bragg grating (FBG 1) at the output of the device suppresses the remaining pump signal by approximately 20 dB. The ring resonator consists of nearly stoichiometric Si_3N_4 grown in multiple layers with intermediate annealing steps [29]. The strip waveguides are patterned with electron beam lithography and transferred to the substrate by reactive ion etching with SF_6/CH_4 chemistry. The waveguides are then embedded into a SiO_2 cladding deposited via low-pressure chemical vapor deposition (LPCVD). The waveguides are 2 μm wide and 750 nm high, and the sidewalls are inclined by 12° with respect to the vertical direction (Fig. 2, Inset 1).

The high-temperature growth technique used to fabricate the 750 nm thick layers of stoichiometric Si_3N_4 requires annealing at 1200°C . This makes it difficult to fabricate SiN resonators in the framework of standard CMOS processes. One option to overcome these limitations is to use dedicated fabrication processes and multi-chip integration as illustrated in Fig. 1. Alternatively, it is possible to deposit Si_3N_4 at 400°C and to use UV thermal processing (UVTP) at lower temperatures to reduce the defect density. Both techniques are subject to ongoing research.

The free spectral range (FSR) of the current resonator samples amounts to 17 GHz, but can be also designed to match standard WDM grids with, e.g., 12.5 GHz or 25 GHz line spacing. The resonator exhibits a loaded Q-factor of 8×10^5 . We expect that improvements in fabrication will allow to increase the Q-factor and hence to decrease the pump power in future experiments. Moreover, microresonators with improved Q-factors will enable generation of broadband frequency combs with hundreds of lines that cover optical bandwidths of hundreds of nanometers - a multiple of what can be achieved with state-of-the-art distributed-feedback WDM laser arrays in InGaAsP technology. Note that in the envisaged system illustrated in Fig. 1, the use of FBG for pump light suppression will become superfluous: If the frequency comb is extracted by a second waveguide coupled to the ring resonator, direct through-coupling of strong cw pump light is not possible, and FBG notch filters are not needed.

Generation of low phase-noise Kerr combs.

To obtain low phase-noise Kerr combs, the pump parameters are adjusted in two steps using the setup depicted in Fig. 2: First, the pump wavelength is periodically scanned across the resonance at a frequency of approximately 100 Hz while staying within the stop band of FBG 2 and continuously measuring the power conversion to the spectral region outside the stop band. During

these scans the polarization of the pump signal is slowly varied to maximize the conversion. Maintaining this polarization, the detuning of the pump signal with respect to the resonance wavelength is then carefully adjusted until the initially broad RF spectrum (Fig. 2, Inset 3) exhibits a single narrow peak (Fig. 2, Inset 4). Note that the frequency axes of Insets 3 and 4 have different scales. The power spectrum of Inset 3 was recorded with a resolution bandwidth (RBW) of 10 kHz whereas Inset 4 was recorded with a RBW of 30 kHz. For an on-chip pump power of approximately 33 dBm the essential part of the optical comb spectrum is depicted in Inset 5 of Fig. 2. From this partial spectrum we selected the lines for our data transmission experiments.

To maintain low-phase noise comb states during the data transmission, it was crucial to keep the pump conditions as constant as possible. The efficiency of fibre-chip coupling turned out to be one of the most crucial parameters in these experiments: The comb state is stabilized by thermal locking of the cavity resonance to the pump wavelength [37], and the associated equilibrium of the nonlinear pump-microcavity system is very sensitive with respect to fluctuations of the on-chip pump power. It was therefore important to continuously monitor and correct the fibre-chip coupling efficiency, thereby keeping the on-chip pump power constant to approximately $\pm 5\%$. We expect that increasing the Q-factors in future devices will not affect the fundamental sensitivity of the comb generation process with respect to pump power fluctuations.

The on-chip pump power needed for Kerr comb generation in this experiment still amounts to 33 dBm. However, there is considerable room for future improvements: The threshold for Kerr comb generation scales inversely quadratic with the Q-factor of the resonator [38]. Hence, a Q improvement of only a factor of 10 would lead to a reduction of the pump power by a factor of 100 and thus replace the 2 Watt pump laser by 20 mW pump laser diode. Kerr combs have been demonstrated with a threshold power as low as 50 μW in silica toroids [2].

Signal impairment analysis.

The optical carrier-to-noise-density ratio (OCN_0R) is limited by the ASE noise originating from the pump amplifier. To determine the OCN_0R , we need to estimate the noise power density right at the frequency of the respective comb line. This is done by averaging the spectral power densities obtained in the middle between two comb lines. The spectral power densities were measured with an optical spectrum analyser (Ando AQ 6317B) in a 0.01 nm bandwidth and renormalized to a bandwidth of 1 Hz.

To improve the signal quality, it is possible to filter out ASE by using a band-pass filter before the DUT. When performing the experiment, however, we did not have any filters that could safely handle the 37 dBm of pump power

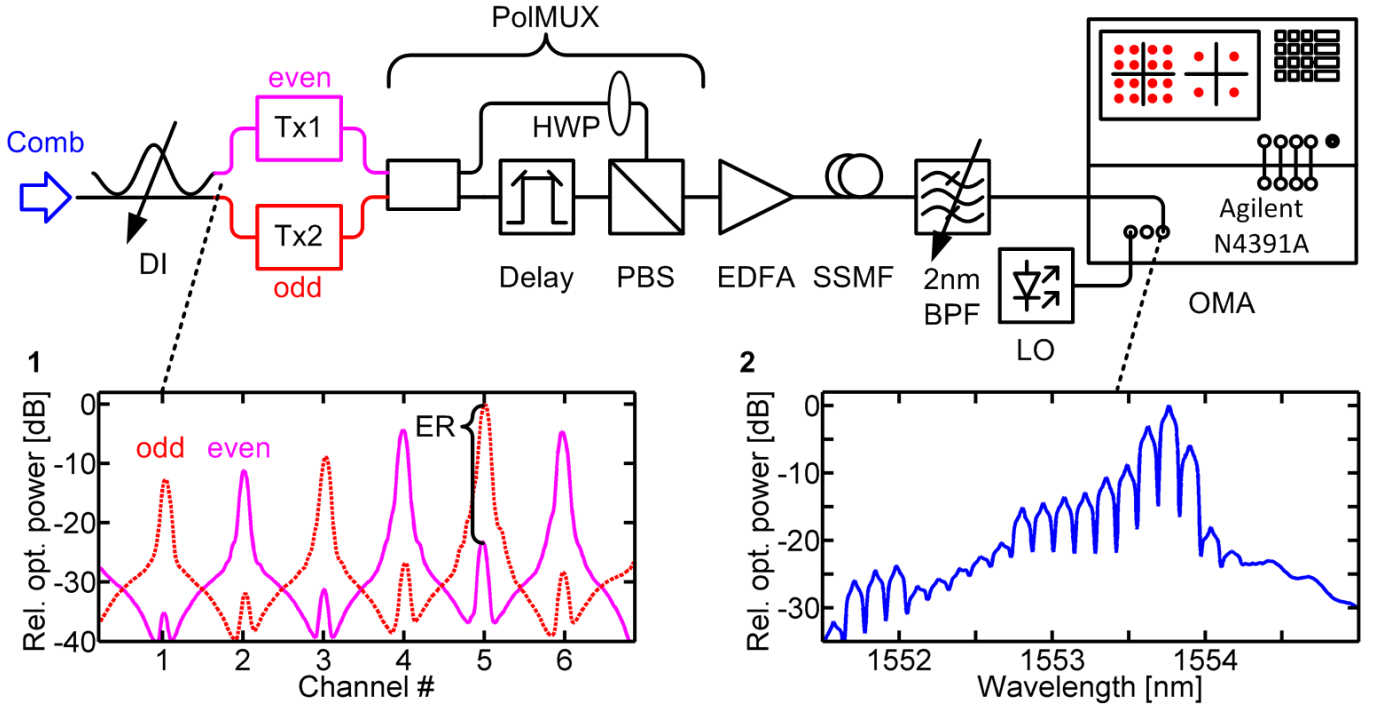


FIG. 4: **Data transmission setup.** A tunable delay interferometer (DI) is used to separate the incoming frequency comb into carriers that belong to odd and even channels. The two sets of channels are then separately modulated at a symbol rate of 14 GBd using QPSK or 16QAM signals and Nyquist sinc-pulses. The two data streams are merged and fed into a polarization multiplexer (PolMUX), comprising a half-wave plate (HWP), a delay line and a polarization beam splitter (PBS). The PolMUX splits the optical signal in two parts, delays one of them to form two uncorrelated data streams, and recombines them on two orthogonal polarization states of the standard single-mode transmission fibre (SSMF). The receiver comprises an erbium-doped fibre amplifier (EDFA), an optical band-pass filter (BPF), and an optical modulation analyzer (OMA) with a tunable laser serving as a local oscillator (LO). Digital signal processing in the baseband is used to separate the WDM channels and to demultiplex the polarizations. Insets: **1**, Spectra of the unmodulated carriers after separation by the DI. Even channels are represented by the magenta solid line, odd channels by the red dotted line. The extinction ratio is better than 20 dB for all channels; **2**, Optical spectrum at the input of the OMA, after the 2 nm band-pass filter. The pronounced noise background predominantly originates from the ASE of the pump EDFA that is used for frequency comb generation.

right after the EDFA. We expect that by further optimizing the fabrication process, we can increase the microresonator's Q-factor and hence significantly decrease the required threshold power [38], such that filtering of the pump signal will be straightforward. In addition the comb may be extracted by a second waveguide which is coupled to the microresonator, see Fig. 1. This avoids direct transmission of broadband ASE noise transmitted through the resonator device. Using resonators with higher Q-factor, it might even be possible to use a high-power pump laser diode without requiring amplification at all.

Supplementary Information

To emulate a WDM communication system, we transmit data on all channels simultaneously, using one pseudo-random bit sequence (PRBS) on the even channels and another independent PRBS on the odd channels. Neighbouring channels hence carry uncorrelated

data streams, and inter-channel crosstalk translates directly into a degradation of signal quality. The corresponding setup is depicted in Fig. 4. Carriers belonging to odd and even channels are first separated by a tunable delay interferometer (DI) [39]. The superposition of both spectra is displayed in Inset 1 of Fig. 4. Two home-built multi-format transmitters [40] are then used to encode QPSK or 16QAM signals with a symbol rate of 14 GBd on the sets of even and odd carriers using independent PRBS with a length of $2^{15} - 1$. Polarization-division multiplexing (PDM) is emulated by splitting the optical signal, and recombining the original and a sufficiently delayed copy to form two decorrelated data streams on orthogonal polarizations. The data stream is transmitted to the receiver, where the signal is amplified, filtered and coherently detected using an optical modulation analyser (OMA, Agilent N 4391 A) with a standard tunable laser (Agilent 81680A) acting as a local oscillator (LO). An optical bandpass filter with a 2 nm passband is used to avoid saturation of the receiver photodiodes. Individual WDM channels are selected by appropriate choice of the

LO wavelength and by digital brick-wall filtering in the baseband. Inset 2 of Fig. 4 shows the optical spectrum at the input of the OMA. The effect of the 2 nm band-pass filter is clearly visible; the noise in the pass-band predominantly originates from the ASE of the pump EDFA that is used for frequency comb generation.

Digital post-processing comprises demultiplexing of the polarization channels, compensation of the frequency offset between the LO and the optical carrier, clock recovery, and equalization. For performance evaluation we use the error-vector magnitude (EVM) metric, which describes the effective distance of a received complex symbol from its ideal position in the constellation diagram. Provided that the signal is impaired by additive white Gaussian noise only, the EVM is directly related [33] to the bit-error ratio (BER). For 16QAM, we estimate a BER of 3×10^{-4} from the measured EVM of 10 %, which is in fair agreement with the measured BER of

7.5×10^{-4} . This confirms the validity of the EVM-based estimation of the BER in our experiment. For the other QPSK channels, the BER of 3×10^{-7} , 7×10^{-8} , 1×10^{-8} , 1×10^{-11} , and 5×10^{-20} are estimated accordingly from the measured EVM values of 20 %, 19 %, 18 %, 15 %, and 11 %.

Apart from the ASE of the pump EDFA as discussed in the Methods Section, we investigated coherent crosstalk as a potential source of signal degradation: The tunable DI used to separate the carriers has a finite extinction ratio (ER), see Inset 1 in Fig. 4. As a consequence, the data signals of the even channels are superimposed by residual carriers modulated with odd-channel data and vice versa, which leads to further signal degradation. However, in our experiment this effect was not relevant: With an ER better than (22.2 ± 1.5) dB for all channels, no correlation of channel ER and EVM can be observed.

-
- [1] Hillerkuss, D. *et al.* 26 Tbit/s line-rate super-channel transmission utilizing all-optical fast Fourier transform processing. *Nature Photon.* **5**, 364–371 (2011).
 - [2] Del’Haye, P. *et al.* Optical frequency comb generation from a monolithic microresonator. *Nature* **450**, 1214 – 1217 (2007).
 - [3] Levy, J. *et al.* High-performance silicon-nitride-based multiple-wavelength source. *IEEE Photon. Technol. Lett.* **24**, 1375–1377 (2012).
 - [4] Herr, T. *et al.* Universal formation dynamics and noise of Kerr-frequency combs in microresonators. *Nature Photon.* **6**, 480–487 (2012).
 - [5] Pfeifle, J. *et al.* Microresonator-Based Optical Frequency Combs for High-Bitrate WDM Data Transmission. In *Optical Fiber Communication Conference*, paper OW1C.4 (OSA, 2012).
 - [6] Wang, P.-H. *et al.* Observation of correlation between route to formation, coherence, noise, and communication performance of Kerr combs. *Opt. Express* **20**, 29284–29295 (2012).
 - [7] Li, J., Lee, H., Chen, T. & Vahala, K. J. Low-Pump-Power, Low-Phase-Noise, and Microwave to Millimeter-Wave Repetition Rate Operation in Microcombs. *Phys. Rev. Lett.* **109**, 233901 (2012).
 - [8] Herr, T., Brasch, V., Gorodetsky, M. L. & Kippenberg, T. J. Mode-locking in an optical microresonator via soliton formation. Preprint at <http://arxiv.org/abs/1211.0733> (2012).
 - [9] Okawachi, Y. *et al.* Octave-spanning frequency comb generation in a silicon nitride chip. *Opt. Lett.* **36**, 3398–3400 (2011).
 - [10] Miller, D. Device requirements for optical interconnects to silicon chips. *Proc. IEEE* **97**, 1166 –1185 (2009).
 - [11] Qian, D. *et al.* 101.7-Tb/s (370×294-Gb/s) PDM-128QAM-OFDM Transmission over 3×55-km SSMF using Pilot-based Phase Noise Mitigation. In *Optical Fiber Communication Conference*, paper PDPB5 (OSA, 2011).
 - [12] Liu, A. *et al.* Wavelength Division Multiplexing Based Photonic Integrated Circuits on Silicon-on-Insulator Platform. *IEEE J. Sel. Top. Quant.* **16**, 23 –32 (2010).
 - [13] Hochberg, M. & Baehr-Jones, T. Towards fabless silicon photonics. *Nature Photon.* **4**, 492–494 (2010).
 - [14] Feng, D., Qian, W., Liang, H., Luff, J. & Asghari, M. High Speed Receiver Technology on the SOI Platform. *IEEE J. Sel. Top. Quant.* **19**, 3800108 (2013).
 - [15] Nagarajan, R. *et al.* InP photonic integrated circuits. *IEEE J. Sel. Top. Quant.* **16**, 1113–1125 (2010).
 - [16] Park, H., Fang, A., Kodama, S. & Bowers, J. Hybrid silicon evanescent laser fabricated with a silicon waveguide and III-V offset quantum wells. *Opt. Express* **13**, 9460–9464 (2005).
 - [17] Fang, A. W., Lively, E., Kuo, Y.-H., Liang, D. & Bowers, J. E. A distributed feedback silicon evanescent laser. *Opt. Express* **16**, 4413–4419 (2008).
 - [18] Lindenmann, N. *et al.* Photonic wire bonding: A novel concept for chip-scale interconnects. *Opt. Express* **20**, 17667–17677 (2012).
 - [19] Dong, P., Chen, L., Xie, C., Buhl, L. L. & Chen, Y.-K. 50-Gb/s silicon quadrature phase-shift keying modulator. *Opt. Express* **20**, 21181–21186 (2012).
 - [20] Korn, D. *et al.* Silicon-organic hybrid (SOH) IQ modulator using the linear electro-optic effect for transmitting 16QAM at 112 Gbit/s. *Opt. Express* **21**, 13219–13227 (2013).
 - [21] Witzens, J. WDM telecommunications link with coherent detection and optical frequency comb sources, WIPO Patent No. 2012150197 (2012).
 - [22] Witzens, J., Baehr-Jones, T. & Hochberg, M. Silicon photonics: On-chip OPOs. *Nature Photon.* **4**, 10–12 (2010).
 - [23] Hillerkuss, D. *et al.* Single-Laser 32.5 Tbit/s Nyquist WDM Transmission. *J. Opt. Commun. Netw.* **4**, 715–723 (2012).
 - [24] Wu, R., Supradeepa, V. R., Long, C. M., Leaird, D. E. & Weiner, A. M. Generation of very flat optical frequency combs from continuous-wave lasers using cascaded intensity and phase modulators driven by tailored radio frequency waveforms. *Opt. Lett.* **35**, 3234–3236 (2010).
 - [25] Rosales, R. *et al.* InAs/InP Quantum-Dot Passively Mode-Locked Lasers for 1.55-μm Applications. *IEEE J.*

- Sel. Top. Quant.* **17**, 1292–1301 (2011).
- [26] Kippenberg, T. J., Holzwarth, R. & Diddams, S. A. Microresonator-Based Optical Frequency Combs. *Science* **332**, 555–559 (2011).
 - [27] Savchenkov, A. A. *et al.* Tunable Optical Frequency Comb with a Crystalline Whispering Gallery Mode Resonator. *Phys. Rev. Lett.* **101**, 093902 (2008).
 - [28] Razzari, L. *et al.* CMOS-compatible integrated optical hyper-parametric oscillator. *Nature Photon.* **4**, 41–45 (2010).
 - [29] Levy, J. S. *et al.* CMOS-compatible multiple-wavelength oscillator for on-chip optical interconnects. *Nature Photon.* **4**, 37–40 (2010).
 - [30] Pfeifle, J. *et al.* Microresonator-Based Frequency Comb Generator as Optical Source for Coherent WDM Transmission. In *Optical Fiber Communication Conference*, paper OW3C.2 (OSA, 2013).
 - [31] Foster, M. A. *et al.* Silicon-based monolithic optical frequency comb source. *Opt. Express* **19**, 14233–14239 (2011).
 - [32] Schmogrow, R. *et al.* Real-time Nyquist pulse generation beyond 100 Gbit/s and its relation to OFDM. *Opt. Express* **20**, 317–337 (2012).
 - [33] Schmogrow, R. *et al.* Error Vector Magnitude as a Performance Measure for Advanced Modulation Formats. *IEEE Photon. Technol. Lett.* **24**, 61–63 (2012). Correction: *ibid.*, 24, 2198 (2012).
 - [34] Chang, F., Onohara, K. & Mizuochi, T. Forward error correction for 100 G transport networks. *IEEE Commun. Mag.* **48**, S48–S55 (2010).
 - [35] Essiambre, R.-J., Kramer, G., Winzer, P., Foschini, G. & Goebel, B. Capacity Limits of Optical Fiber Networks. *J. Lightw. Technol.* **28**, 662–701 (2010).
 - [36] Bozinovic, N. *et al.* Terabit-Scale Orbital Angular Momentum Mode Division Multiplexing in Fibers. *Science* **340**, 1545–1548 (2013).
 - [37] Carmon, T., Yang, L. & Vahala, K. Dynamical thermal behavior and thermal self-stability of microcavities. *Opt. Express* **12**, 4742–4750 (2004).
 - [38] Kippenberg, T. J., Spillane, S. M. & Vahala, K. J. Kerr-Nonlinearity Optical Parametric Oscillation in an Ultrahigh-Q Toroid Microcavity. *Phys. Rev. Lett.* **93**, 083904 (2004).
 - [39] Li, J. *et al.* Free-space optical delay interferometer with tunable delay and phase. *Opt. Express* **19**, 11654–11666 (2011).
 - [40] Schmogrow, R. *et al.* Real-Time Software-Defined Multiformat Transmitter Generating 64QAM at 28 GBd. *IEEE Photon. Technol. Lett.* **22**, 1601–1603 (2010).